

# Fluid-structure coupled computations of the NREL 5MW wind turbine blade during standstill

**B. Dose<sup>1</sup>, H. Rahimi<sup>1</sup>, I. Herráez<sup>1</sup>, B. Stoevesandt<sup>2</sup>, J. Peinke<sup>1,2</sup>**

<sup>1</sup> ForWind, Institute of Physics, University of Oldenburg, Ammerländer Heerstr.114-118, 26129 Oldenburg, Germany

<sup>2</sup> Fraunhofer IWES, Ammerländer Heerstr.136, 26129 Oldenburg, Germany

E-mail: [bastian.dose@uni-oldenburg.de](mailto:bastian.dose@uni-oldenburg.de)

## Abstract.

This work is aimed at investigating the aero-elastic behavior of a wind turbine blade subjected to strong wind speeds during standstill. This type of investigation still remains a challenge for most wind turbine simulation codes. For this purpose, a new developed high fidelity framework for fluid-structure coupled computations of wind turbines is presented and numerical simulations are conducted on the NREL 5MW reference wind turbine. The framework couples the open-source Computational Fluid Dynamics (CFD) toolbox OpenFOAM with an in-house beam solver, based on the Geometrically Exact Beam Theory (GEBT). The obtained results are compared to the aero-elastic tool FAST, which is based on the Blade Element Momentum theory (BEM) and can be considered as a state-of-the-art wind turbine simulation code. The evaluation of the fluid-structure coupled CFD simulations reveals clear differences in the results compared to FAST. While the mean deflections show a reasonable agreement, the dynamics of the edgewise deflections differ significantly. Furthermore, the effect of an explicit coupling versus an implicit coupling strategy on the results is investigated.

## 1. Introduction

Over the last decades a clear trend towards larger and more flexible rotor designs emerged. This trend makes modern wind turbines very sensitive to aero-elastic influences. As an example, one critical load case is the standstill case, which can occur during the erection of a wind turbine, during operation due to failure of the blade yaw system or at idling conditions. According to the IEC 61400-1 guideline [1], in this load case the blades have to withstand extreme wind speeds from different directions. Due to the high angles of attack and therefore often fully separated flows in combination with a strong interaction of the flow and the structure, the standstill load case is numerically complex to simulate. Aero-elastic instabilities in the field of wind turbines have been subject to research for many years [2, 3]. One remaining issue is the modeling of the instationarity of the aerodynamics, which is required by aerodynamic models of lower fidelity like the Blade Element Momentum theory (BEM). To avoid this issue, CFD is increasingly used to simulate elastically mounted, extruded airfoil sections (3D) for investigating the phenomena occurring at standstill [4, 5]. Recently, Heinz et al. published a study on vortex-induced vibrations performed on the DTU 10 MW research wind turbine blade [6]. The fluid-structure coupled simulations were conducted on the three-dimensional blade geometry using the aero-elastic tool HAWC2CFD [7], which couples the wind turbine simulation code HAWC2 [8] with



the CFD code EllipSys3D [9]. They reported that under certain conditions, already relatively low or moderate wind speeds were able to trigger significant vibrations of the investigated blade.

In this work, a new developed high-fidelity framework is presented and used for fluid-structure coupled computations on a multi-Megawatt wind turbine blade at standstill. In addition, the same conditions are simulated using the aero-elastic BEM-based code FAST [10] and the obtained results are compared to the coupled CFD.

## 2. Methodology

To capture the Fluid-Structure Interaction (FSI), the open source CFD code OpenFOAM [11] is coupled to an in-house structural solver based on Finite Elements (FE), which is directly implemented into the OpenFOAM framework. The following sections provide an overview about the used methods, the coupling of the latter and the implemented mesh update algorithm.

### 2.1. Flow Solver

The solving of the flow domain is performed using the open source CFD toolbox OpenFOAM 2.4.0 [11]. To reach a compromise between the accuracy of Large Eddy Simulations (LES) and the computationally more economical Unsteady Reynolds-averaged Navier-Stokes (URANS) simulations, incompressible Delayed Detached Eddy Simulations (DDES) are performed. The DDES approach available in OpenFOAM [12] utilizes the one equation RANS turbulence model by Spalart and Allmaras [13] near the wall, and LES for the rest of the domain. Due to the URANS modeling approach in the vicinity of the wall, the time resolution does not need to be as high like in the case of a pure LES simulation. Nevertheless, large eddies in the wake are resolved. This is expected to increase the accuracy of the numerical simulations in regions dominated by large eddies, which is the case in the wake of wind turbine blades.

The coupling of velocity and pressure is performed using the merged SIMPLE-PISO algorithm PIMPLE, which is available in the OpenFOAM package. The convective terms are discretized using the second-order accurate linear-upwind scheme, the discretization in time is performed using a second-order backward formulation.

### 2.2. Structural Solver

The structural response of the wind turbine blade is computed by a new implemented in-house structural beam solver. Using a finite element formulation based on the Geometrically Exact Beam Theory (GEBT), originally proposed by Reissner [14] and extended to 3D by Simo [15], the structural solver is suitable for the investigation of large rotor blades. The geometrical non-linearity ensures a high accuracy for large deformations, the use of full 6x6 cross sectional matrices for stiffness and mass allows to account for complex, anisotropic material layouts and cross sectional couplings like bend-torsion coupling. The current implementation is based on the work of Cardona and G eradin [16, 17]. Iso-parametric beam elements are employed for the spatial discretization, the rotations are parametrized using a Cartesian rotation vector. The code is capable of accounting for gyroscopic effects and centrifugal stiffening. In addition, offsets of the sectional center of gravity from the principal beam axes can be taken into account. To avoid shear locking, reduced integration is utilized. Integration in time is performed using the second-order accurate generalized-alpha scheme [18].

### 2.3. Coupling Approach

The coupling of flow and structural solver is implemented based on a partitioned approach. Fluid and structural domain are solved by independent solvers which allows to couple the structural

solver to different flow solvers within OpenFOAM. As the structural solver is directly embedded into the OpenFOAM's *C++* framework, information transfer between both domains is performed in memory and without the need of external coupling interfaces. To enable the usage of the developed code on multiple computational cores, the framework is parallelized. The solving of the flow domain and the mesh update are performed in parallel, the computation of the structural response is performed in serial. The required computational time for the structural solver lies typically in the range of few tenth of a second per time step. One important aspect of the coupling is the transfer of the aerodynamic forces. Obtained from the blade surface mesh in the fluid domain (3D), the forces have to be transferred to the one-dimensional structural domain. In this work, the aerodynamic forces and moments generated by each face of the corresponding fluid surface mesh are projected onto the beam and its finite elements. Then the projected forces and moments are divided up onto each beam node of the corresponding element using the internal shape functions. After that, they are summed up at each beam node. The coupling of flow and structure solving processes can be performed in an explicit manner (once per time step), or using an implicit coupling strategy (more than once per time step).

#### 2.4. Mesh Update

To avoid computational costly re-meshing and to ensure a computationally efficient and robust mesh update, a suitable mesh motion technique was implemented into OpenFOAM. The method uses a Newton algorithm to project the points of the corresponding surface mesh and all volume mesh points within a selectable distance near the surface onto the structural beam. Assigned to a specific beam element, including the position within the latter and based on its distance to the beam axis, each point is moved according to the deformation of the structure. To preserve first cell heights, growth ratios and cell quality within the structured boundary layer near the geometry, cells within a certain distance around the geometry are translated and rotated rigidly. Between the rigidly moved point zones and fixed outer mesh zones, cubic polynomials are used to smooth out the motion. Figures 1 and 2 illustrate the implemented method for a simple beam. The rigidly moved points are colored in red, the transition zone is colored in grey. The fixed zone is colored white. The structural nodes (within the beam) are marked by circles. The main advantages of this parametric method are its robustness and its low computational costs, as no set of equations needs to be solved for the mesh motion.

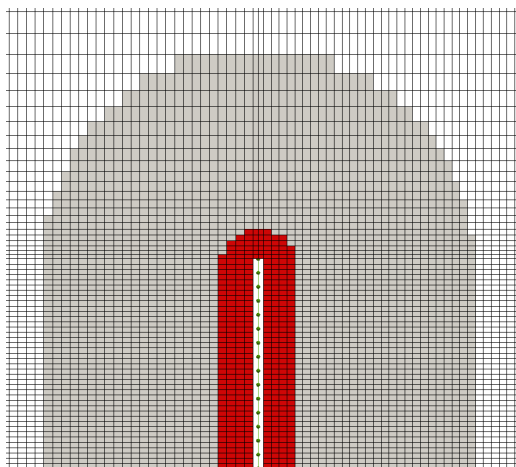


**Figure 1.** Initial example mesh before deformation.

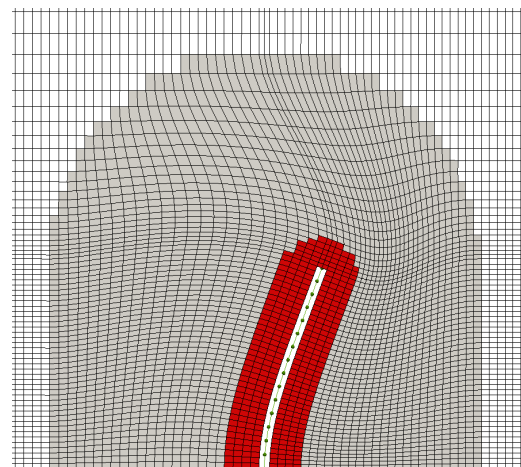


**Figure 2.** Updated example mesh after deformation.

### 3. Validation of the structural solver

To demonstrate the capabilities of the structural solver, two validation cases which are relevant for fluid-structure coupled simulations of wind turbines blades during standstill situations, are presented in this paper. The results are compared to computations performed in the frame of a comparison of the structural models of two aero-elastic simulation codes for wind turbines [19], namely HAWC2 and FAST. The first case presented in this paper is a static test case of an initially twisted straight beam. The beam has a length of  $L = 10m$ , the cross sectional structural properties are given in Ref.[19]. Figures 3 and 4 show the beam structure in its initial configuration and under load. The initial, linear twist of the structure with a twist of  $90^\circ$  at its free end can be observed. The beam is loaded with a force of  $F = 4000kN$  in negative z-direction.

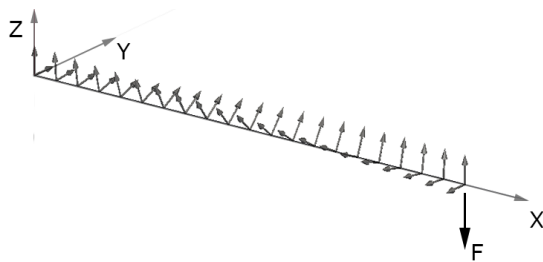


**Figure 3.** Initially twisted beam: Initial configuration.

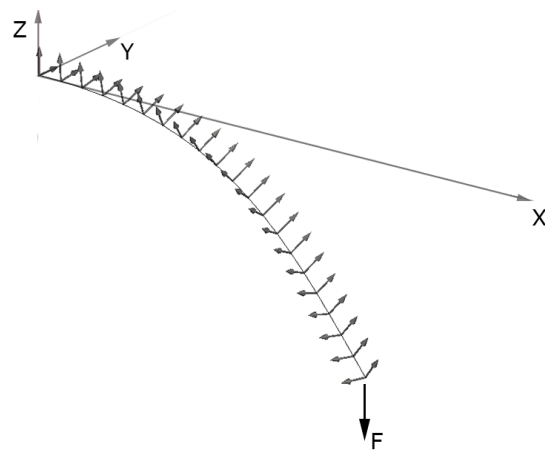


**Figure 4.** Initially twisted beam: Loaded configuration.

The obtained results for the current implementation are shown in table 1. In addition, results obtained by HAWC2 and BeamDyn [20], which is the present structural solver of FAST, are listed. The reference solution is obtained by ANSYS using a refined mesh based on ANSYS SOLID186 elements [19]. A very good agreement can be noticed for the deflections in all directions.

**Table 1.** Comparison of tip displacement for loaded beam.

	$u_x$ [m]	$u_y$ [m]	$u_z$ [m]
ANSYS	-1.134	-1.714	-3.584
BeamDyn	0.13%	0.04%	0.15%
HAWC2	2.42%	1.92%	1.05%
Current	0.52%	0.03%	0.22%

The second validation case presented is a dynamically loaded straight beam, clamped at one side. The length of the beam is given with  $L = 10m$ . At the free end of the beam a dynamic force

$F_z(t) = A_{F_z} \sin(\omega t)$ , with  $A_{F_z} = 100N$  and  $\omega = 10 \frac{rad}{s}$ , is applied. The structural properties can be found in [19]. It is important to mention, that the provided 6x6 stiffness matrix includes a coupling of bending modes and torsional modes. Figure 5 shows the initial configuration of the investigated structure.

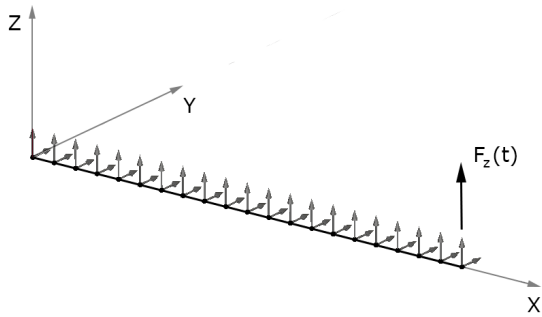


**Figure 5.** Dynamically loaded beam: Initial configuration.

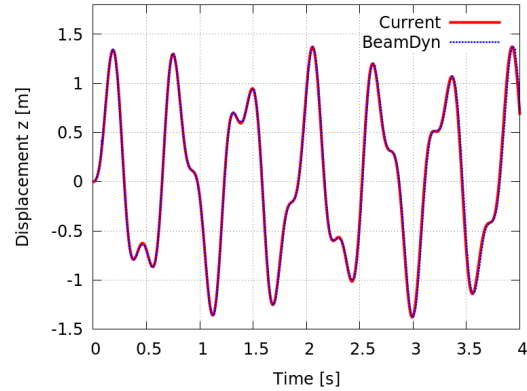


**Figure 6.** Dynamically loaded beam: Displacement at free end in z-direction.

Figures 6, 7 and 8 illustrate the structural response to the dynamic load. The agreement between the current implementation and BeamDyn can be considered as excellent. It can be concluded, that the present structural solver is capable of performing dynamic simulations of beam-like structures as wind turbine blades.

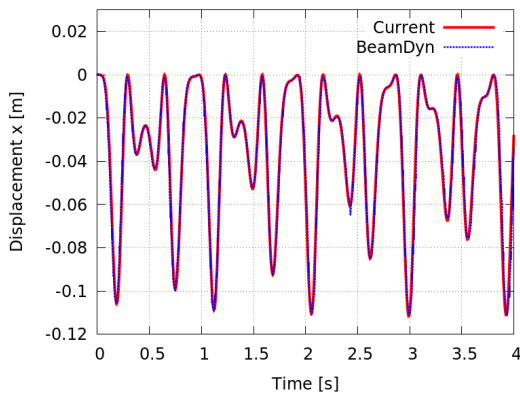


**Figure 7.** Dynamically loaded beam: Displacement at free end in x-direction.

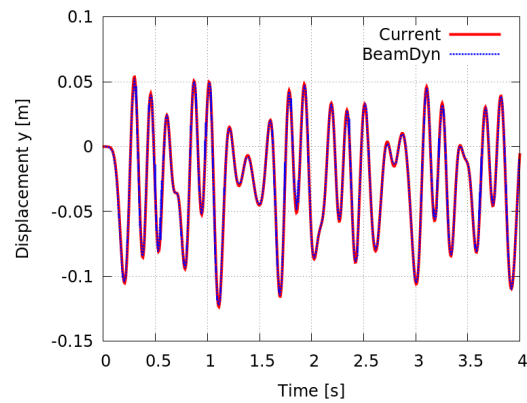


**Figure 8.** Dynamically loaded beam: Displacement at free end in y-direction.

#### 4. Numerical setup

Fluid-structure coupled simulations are performed on the 5MW reference wind turbine, designed by the National Renewable Energy Laboratory (NREL) [21], during standstill. The blade has a length of  $61.5m$  and the blade pitch is fixed to  $0^\circ$ . The fluid domain is discretized using a fully structured, half-spherical grid consisting of 24 million hexahedron cells. The radius of the half sphere accounts to seven blade lengths. Generated using the software Pointwise [22], the mesh is based on 500 cells in span-wise direction, 250 cells in the chord-wise direction and 190 cells normal to the blade surface. Figure 9 illustrates the used computational grid for the flow domain in more detail. Figure 10 shows an example of the mesh resolution near the blade surface. To avoid high cell aspect ratios, adaptive wall functions are used within this work. The structural modeling of the blade is based on the isotropic structural properties provided in Ref.[21] using three-noded iso-parametric elements with quadratic shape functions. Gravitational forces acting on the structure are included within the simulations. The coupling of the flow solver and the structural solver are performed once (explicit) or twice (implicit) per time step. The simulations are performed in parallel using 240 computational cores on the FLOW cluster at the University of Oldenburg.

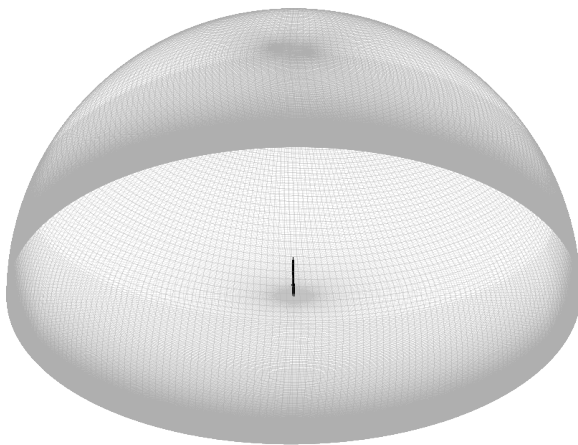


**Figure 9.** Shape of the fluid domain.

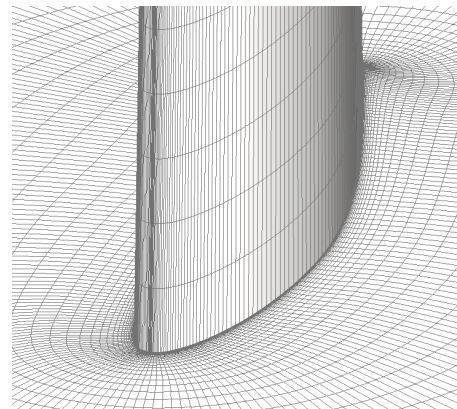


**Figure 10.** Computational grid near the leading edge at  $r/R=75\%$ .

The physical time step of the simulations was selected as  $\Delta t = 5 \cdot 10^{-3}s$ . To avoid unphysical excitations of the structure caused by not converged forces, the fluid-structure coupling is activated first after 10s of simulation time. Before that, the simulated blade geometry is kept rigid. An overview about the conducted simulations is given by table 2.

**Table 2.** Simulated cases using the coupled CFD solver.

	Inflow velocity [ $m/s$ ]	Inflow angle [ $^\circ$ ]	Coupling approach
Case 1	40	90	Explicit
Case 2	50	90	Explicit
Case 3	50	90	Implicit

All simulations are performed using an inflow angle of  $90^\circ$ , resulting in an angle of attack distribution at the blade between  $\approx 77^\circ$  at the root and  $\approx 90^\circ$  at the tip.

The results are compared to simulations conducted using the aero-elastic, BEM-based code FAST, which can be considered as a state of the art BEM code. For the simulations in FAST, the included setup of the 5 MW reference turbine is used. This includes also the use of the provided lift and drag polars.

### 5. Simulation of the NREL 5MW at standstill

The evaluation of the simulations indicates clear differences in the results of both numerical approaches. Figure 11 illustrates the complex turbulent wake behind the NREL 5MW blade during standstill. Shown is an iso-surface for the vortex criterion  $Q$  [23], obtained from the coupled CFD simulation. The large out-of-plane deflection at the beginning of the simulation is clearly visible. The initial geometry is shown in light grey. The instantaneous direction of the wall shear stress on the suction side of the blade near the blade tip at  $t = 20s$  is displayed in figure 12. The fully separated flow and its strong span-wise component can be observed.

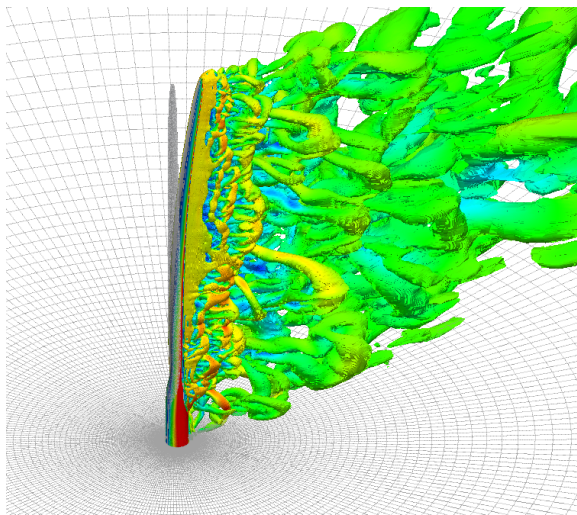


**Figure 11.** Instantaneous isosurface for the vortex criterion  $Q$  [23] coloured by velocity magnitude. The initial blade geometry is shown in grey. Inflow speed: 50m/s, physical time: 1s.



**Figure 12.** Instantaneous direction of wall shear stress on suction side near blade tip. Inflow speed: 40m/s, physical time: 20s.

Figures 13 and 14 show the in- and out-of-plane deflections at the tip of the NREL 5MW reference turbine for an inflow velocity of  $40 \frac{m}{s}$  for both FAST and the fluid-structure coupled CFD approach. It can be observed, that both the mean and extreme values of the in- and out-of-plane deflections are predicted similar. This indicates that the mean forces in normal direction and the forces in the direction of the rotor plane show a good agreement for both approaches. Considering the high inflow angle of the investigated case ( $90^\circ$ ) and the complex flow situation, it can be concluded that BEM can provide useful information about mean and extreme deflections under such complex conditions. Nevertheless, the dynamics of the deflections show clear differences. While in terms of out-of-plane deflections, the fluid-structure coupled CFD solver predicts small, irregular fluctuations around its mean value, FAST predicts a steady out-of-plane deflection without any fluctuations. In the case of in-plane displacements, the result

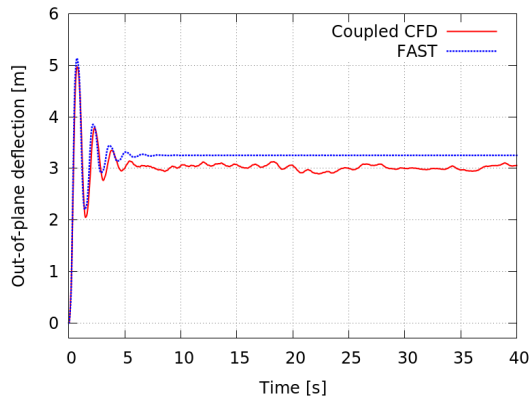


**Figure 13.** Out-of-plane deflection at blade tip for an inflow velocity of  $40 \frac{m}{s}$ .

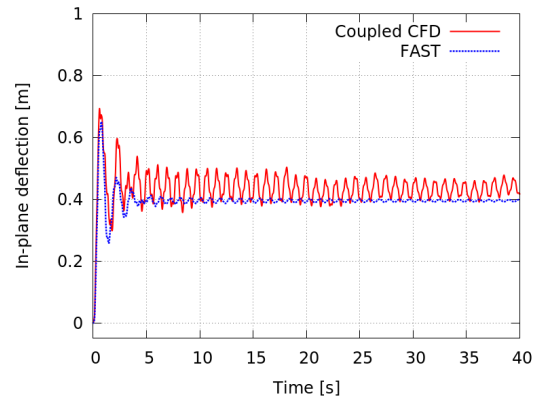


**Figure 14.** In-plane deflection at blade tip for an inflow velocity of  $40 \frac{m}{s}$ .

of the coupled solver shows clear edgewise vibrations of the blade. The peak-to-peak amplitude amounts to  $\approx 0.1m$ , which corresponds to approximately 25% of the mean deflection. In contrast to that, FAST is not able to capture those vibrations. The main reason for this significant difference can be found in the dynamics of the aerodynamic forces. Since BEM is by nature a quasi-steady concept, correction models have to be used to account for complex, transient aerodynamic effects. Based on the authors knowledge, no suitable correction model for BEM-based simulations does currently exist for the dynamics of fully stalled flows at such high angles of attack. Therefore FAST is not able to capture shedding vortices, e.g. the Karman vortex street, which can excite the structure and give rise to blade vibrations. The only available option in FAST to account for dynamics in the lift and drag polars is the Beddoes-Leishman dynamic stall model [24]. However, the model was not developed for such high angles of attack and the changes in angle of attack are rather small. A comparison of simulations with and without the Beddoes-Leishman dynamic stall model in FAST showed that for the investigated cases no difference could be found within the results.

Figure 15 and 16 illustrate the out-of-plane and in-plane tip deflections for an inflow velocity of  $50 \frac{m}{s}$ .

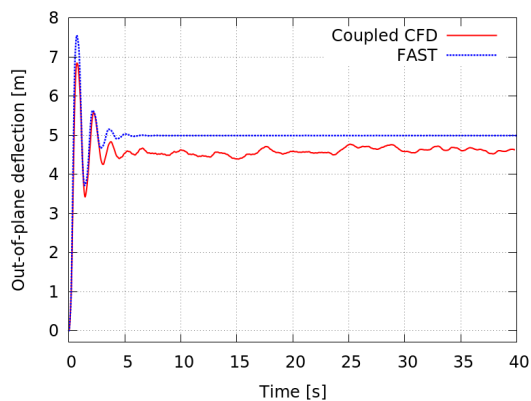


**Figure 15.** Out-of-plane deflection at blade tip for an inflow velocity of  $50 \frac{m}{s}$ .

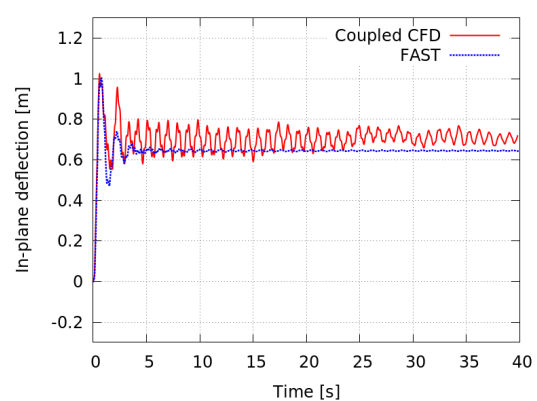


**Figure 16.** In-plane deflection at blade tip for an inflow velocity of  $50 \frac{m}{s}$ .

The comparison of the results confirms the findings obtained from the simulations for the lower velocity. It can be noticed that the amplitude of the edgewise vibrations predicted by the fluid-structured coupled CFD solver, is almost twice as high as for the lower velocity.

In the last part of this work, a comparison of two different coupling approaches is presented. Figures 18 and 17 show the out-of-plane and in-plane deflections for an explicit coupling approach and an implicit coupling approach, where the fluid-structure coupling is performed twice per time step. The implicit coupling is performed without relaxation. Due to the second coupling, the computational costs for simulations using the implicit coupling strategy is almost twice as high. It can be observed that both results are similar and don't show much deviations. The most noticeable difference can be observed in the time frame from 6s – 8s. The out-of-plane vibration shows a small shift in frequency and slightly higher mean value. Nevertheless, the changes can be considered as neglectable. It can therefore be concluded, that the explicit coupling strategy is suitable for the simulated cases.

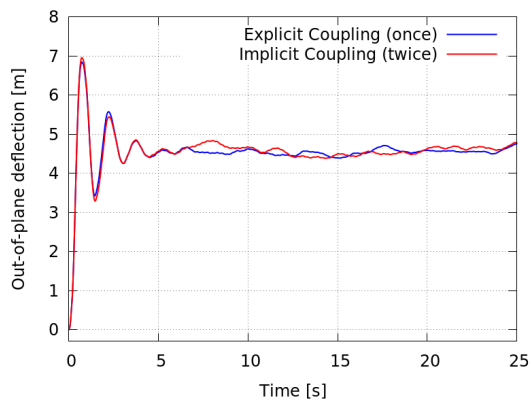


**Figure 17.** Out-of-plane deflection at tip.

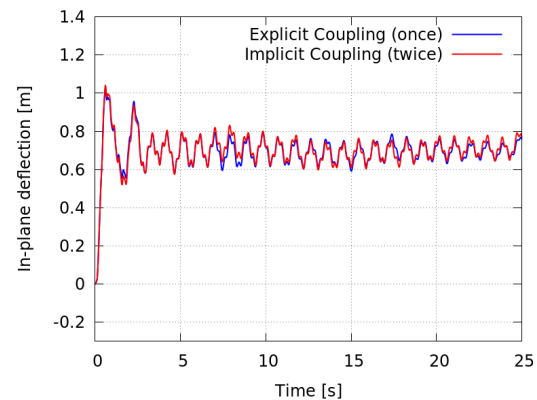


**Figure 18.** In-plane deflection at tip.

## 6. Conclusion

In this paper a new high fidelity framework for fluid-structure coupled computations of modern rotor blades is presented. To prove the capabilities of the implemented structural formulation, the obtained results for two validation cases are compared to state-of-the-art structural models for wind turbine simulations, namely HAWC2 and BeamDyn. Subsequently, fluid-structure coupled computations are performed on the NREL 5MW reference wind turbine blade at standstill for two different wind velocities. The obtained results are compared to the aero-elastic code FAST in terms of the in-plane and out-of-plane displacements at the blade tip. The mean deflections, both in in-plane and out-of-plane direction, show a reasonable agreement. However, significant differences existed in the oscillatory behavior of the structural deformation: Owing to a missing suitable correction model, the BEM-based FAST could not reproduce the vibrations, but showed an almost constant blade tip deflection. Although standstill situations at such high wind velocities are not occurring often in reality, they are part of the IEC 61400-1 guideline since they can lead to significant loads and damage. Based on the evaluated results it has to be stated that computations performed with BEM-based tools on standstill situations should be treated with care. Although the predicted edgewise vibrations at the simulated wind speeds were stable, potential aero-elastic instabilities could not be correctly predicted by a simplified BEM-approach. It was also shown that an implicit coupling procedure with two couplings per time step showed similar results as an explicit coupling with one coupling per time step.

## Acknowledgments

The simulations were performed at the HPC Cluster FLOW (Facility for Large-Scale COmputations in Wind Energy Research), located at the University of Oldenburg (Germany) and funded by the Federal Ministry for the Environment, Nature Conservation and Nuclear Safety (Bundesministerium für Umwelt, Naturschutz und Reaktorsicherheit, BMU) under grant number 0325220.

## References

- [1] IEC 2005 *Wind Turbines - Part 1: Design Requirements, IEC 61400-1 (3rd edn.)* (Genova) ISBN 2-8318-8161-7
- [2] Hansen M H 2007 *Wind Energy* **10** 551–577 ISSN 10954244
- [3] Hansen M H 2003 *Wind Energy* **6** 179–195 ISSN 10954244
- [4] Skrzypiński W R and Gaunaa M 2015 *Wind Energy* **18** 515–527 ISSN 10991824
- [5] Skrzypiński W R, Gaunaa M, Sørensen N N, Zahle F and Heinz J C 2014 *Wind Energy* **17** 1495–1514 ISSN 10991824
- [6] Heinz J C, Sørensen N N, Zahle F and Skrzypiński W R 2016 *Wind Energy* ISSN 1095-4244
- [7] Heinz J C, Sørensen N N and Zahle F 2016 *Wind Energy* ISSN 1099-1824
- [8] Kim T, Hansen A M and Branner K 2013 *Renewable Energy* **59** 172–183 ISSN 09601481
- [9] Sørensen N 1995 *General purpose flow solver applied to flow over hills* Ph.D. thesis published 2003
- [10] Jonkman J 2013 *51st AIAA Aerospace Sciences Meeting, Grapevine Texas* January ISBN 9781624101816
- [11] 2015 OpenFOAM® - The Open Source Computational Fluid Dynamics (CFD) Toolbox URL <http://www.openfoam.com/>
- [12] Spalart P R, Deck S, Shur M L, Squires K D, Strelets M K and Travin A 2006 *Theoretical and Computational Fluid Dynamics* **20** 181–195 ISSN 09354964
- [13] Spalart P R and Allmaras S R 1994 *La Recherche Aérospatiale* **1** 5–21 ISSN 00341223
- [14] Reissner E 1972 *Zeitschrift für angewandte Mathematik und Physik* **23** 795–804 ISSN 00442275
- [15] Simo J 1985 *Computer Methods in Applied Mechanics and Engineering* **49** 55–70 ISSN 00457825
- [16] Cardona A and Géradin M 1988 *International Journal For Numerical Methods in Engineering* **26** 2403–2438 ISSN 0029-5981
- [17] Géradin M and Cardona A 2001 Flexible Multibody Dynamics, A Finite Element Approach
- [18] Arnold M and Brüls O 2007 *Multibody System Dynamics* **18** 185–202 ISSN 1384-5640
- [19] Pavese C, Wang Q, Kim T, Jonkman J and Sprague M 2015 *HAWC2 and BeamDyn: Comparison Between Beam Structural Models for Aero-Servo-Elastic Frameworks* (European Wind Energy Association (EWEA)) paper for poster presentation
- [20] Wang Q, Sprague M, Jonkman J and Johnson N 2015 BeamDyn : A High-Fidelity Wind Turbine Blade Solver in the FAST Modular Framework Preprint Tech. rep.
- [21] Jonkman J, Butterfield S, Musial W and Scott G 2009 Definition of a 5-MW reference wind turbine for offshore system development Tech. rep.
- [22] 2016 Pointwise URL [www.pointwise.com](http://www.pointwise.com)
- [23] Hunt J C R, Wray A A and Moin P 1988 *Center for Turbulence Research, Proceedings of the 1988 Summer Program on Studying Turbulence Using Numerical Simulation Databases (SEE N89-24538 18-34)* 193–208
- [24] Leishman J and Beddoes T 1989 *Journal of the American Helicopter Society* **34** 3–17